Materials Science and Engineering B 176 (2011) 45–48

Contents lists available at ScienceDirect

Materials Science and Engineering B

journal homepage: www.elsevier.com/locate/mseb

Design of porous silicon/PECVD SiO_x antireflection coatings for silicon solar cells

L. Remache[a,*], E. Fourmond[a], A. Mahdjoub[b], J. Dupuis[a], M. Lemiti[a]

[a] Institut des Nanotechnologies de Lyon INL, CNRS-UMR5270, Université de Lyon, INSA-Lyon, Villeurbanne F-69621, France
[b] Laboratoire LMSSEF, Université d'Oum El Bouaghi, Algeria

ARTICLE INFO

Article history:
Received 28 January 2010
Received in revised form 20 June 2010
Accepted 28 August 2010

Keywords:
Porous silicon
Silicon dioxide
Antireflection coating
Photocurrent

ABSTRACT

The meso-porous silicon (PS) has become an interesting material owing to its potential applications in many fields, including optoelectronics and photovoltaics. PS layers were grown on the front surface of the n^+ emitter of n^+–p mono-crystalline Silicon junction. The thickness and the porosity of the PS layer were determined by an ellipsometer, as a function of time duration of anodization, and the variation law of the PS growth kinetics is established. Single layers PS antireflection coating (ARC) achieved around 9% of effective reflectivity in the wavelength range between 400 and 1000 nm on junction n^+–p solar cells. To reduce the reflectivity and improve the stability and passivation properties of PS ARC, silicon oxide layers were deposited by PECVD on PS ARC. SiO_x layers of thickness of 105 nm combined with PS layer led to 3.8% effective reflectivity. V_{oc} measurements were carried out on all the samples by suns-V_{oc} method and showed an improvement of the quality of the passivation brought by the oxide layer. Using the experimental reflectivity results and taking into account the passivation quality of the samples, the PC1D simulations predict an enhancement of the photogenerated current exceeding 44%.

1. Introduction

To reduce the front surface reflectance of crystalline silicon (Si) solar cells is one of the most important point to improve the cells efficiency. Several research groups have used porous silicon (PS) layers as an antireflection coating to reduce the surface reflectance [1–4]. The refractive index of PS layers depends on its porosity and its morphology, and the optimization of these factors may lead to an ideal antireflection coating for silicon solar cells [5]. Porous silicon possesses other advantages and can also (i) enlarge the spectral sensitivity region [6], (ii) improve photo-generation of carriers [6–8], (iii) create simultaneously a selective emitter and an antireflection coating in the same step [6,9]. However, the surface recombination velocity strongly increases when using PS layers, due to the roughness of the surface [10–12]. The optical properties of PS layers may also degrade in time when no further treatment is used [13–15], such as rapid thermal oxidation (RTO), nitridation, anodic oxidation, thermal carbonization [6,16]. In this context silicon oxide (SiO_x) films deposited by PECVD on the porous silicon surface are of interest, since they have good properties: (i) high chemical stability [16–18], (ii) acceptable passivation of the surface after annealing [19,20], (iii) refractive indexes suitable for antireflection coating and (iv) deposition by a low thermal process (plasma enhanced CVD) on the PS surface, without degradation of the optical and structural properties of the underlying PS [17,21].

This work aims to study the optical and the surface passivation properties of PS and PS/SiO_x combinations on n^+/p junction. PS layers were grown electrochemically, the n^+/p junctions were obtained using phosphorous diffusion from $POCl_3$ source at low pressure, and the SiO_x layers were deposited by RF-PECVD.

2. Experimental

The experiments were carried out on CZ (1 0 0) P-type silicon substrates, with a bulk resistivity of 1–10 Ω cm. The emitter was created by diffusion at 850 °C for 20 min, in an open quartz tube using liquid $POCl_3$ as the doping source. This resulted in the formation of an emitter with a sheet resistance of 45 Ω/□. The junction depth was around 0.3 μm. After diffusion the phosphorus silicate glass were removed in dilute HF, and the parasitic junction on the border of the cell was removed by laser beam etching. In order to allow homogeneous electrochemical porosification of the silicon surface, an aluminum layer was evaporated under vacuum on the back side of the sample and was subsequently annealed in air at 750 °C to establish an ohmic contact. This Al back contact was connected to a constant current source. PS was thus grown on the emitter by using a solution of HF (48%) and C_2H_5OH (3:1 or 4:1 in volume) in a Teflon electrochemical anodization cell. A platinum wire was used as a cathode at a distance of 2 cm from the Si wafer surface, which acted as the anode. In order to grow PS lay-

* Corresponding author. Tel.: +33 04 72 43 82 33; fax: +33 04 72 43 85 31.
E-mail address: rlouardi@yahoo.fr (L. Remache).

0921-5107/$ – see front matter © 2010 Elsevier B.V. All rights reserved.
doi:10.1016/j.mseb.2010.08.010

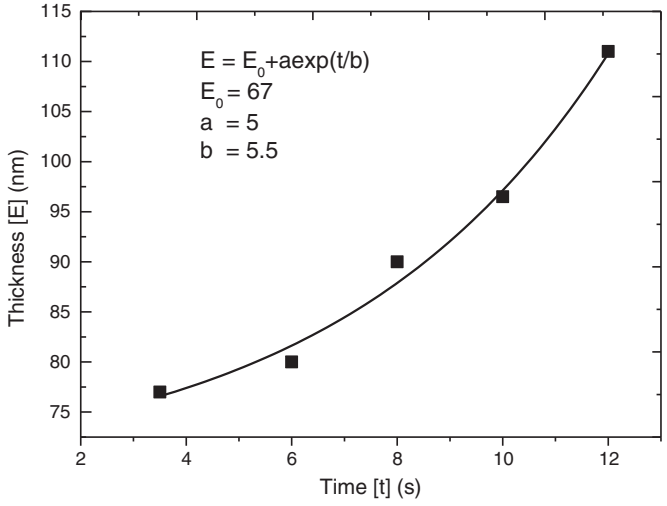

Fig. 1. Thickness E vs anodization time t of PS growth at a constant current density of 20 mA cm^{-2} on n$^+$ diffused side of (1 0 0) Si wafer.

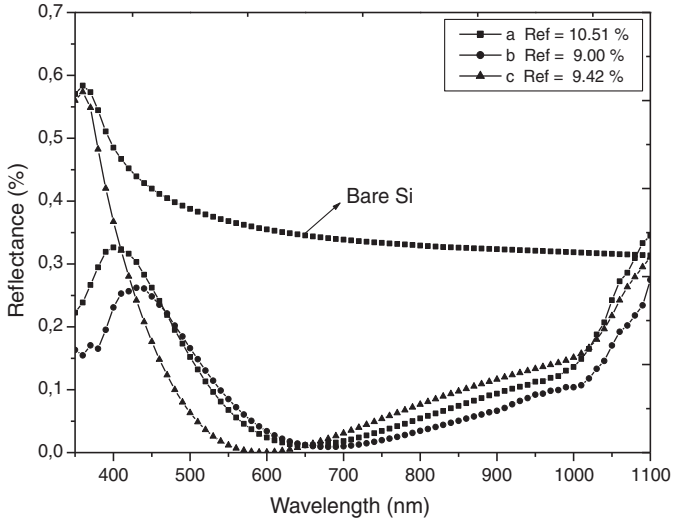

Fig. 2. Total reflectance spectra of: (a) PS growth in HF (48%): C_2H_5OH = 3:1, J = 20 mA/cm^2, t = 6 s; (b) HF (48%): C_2H_5OH = 4:1, J = 20 mA/cm^2, t = 6 s; (c) standard SiN_x ARC (73 nm).

ers with different thicknesses, a set of experiments was performed by using a constant current density of 20 mA/cm^2 during different anodization time: 3.5–12 s. The PS wafers were then cleaned by a standard CARO procedure. SiO_x films were deposited with pure silane and nitrous oxide (SiH_4, N_2O) as precursors gases in a vertical semi-industrial, low frequency PECVD reactor (LF-PECVD) at 440 kHz from SEMCO engineering (described in [22]). The deposition was made at 370 °C, with a power density of 0.26 W/cm^2, a pressure of 1500 mTorr, and a N_2O/SiH_4 gas flow ratio equal to 25. The deposition rate is 29 nm/s.

In order to optimize the ARC parameters (optical indexes and thicknesses), simulations based on the stratified medium theory and the Bruggeman effective medium approximation (EMA) [23] are carried out in the wavelength range between 350 and 1100 nm. The PC1D software was used to estimate the expected values of the photocurrent solar cells [24].

The PS thickness and porosity, and the oxide thickness were measured by a Jobin Yvon Uvisel Ellipsometer, using the Bruggemann effective medium approximation model (EMA) in the range of 1.5–5 eV. The total reflectance was measured within the 350–1100 nm wavelength range with an integrating sphere. The effective reflectance is calculated by integrating the reflectivity values balanced by the Sun global irradiance (AM1.5 g spectrum). The front side metallization of the solar cells was made by evaporation of Ti/Pd/Ag contacts, followed by a sintering step in air at 450 °C. The measurement of the photovoltaic pseudo-parameters (open circuit voltage V_{oc} and pseudo-fill-factor, FF) was carried out using a Sinton Suns-V_{oc} Stage model WCT-120.

3. Optical results

3.1. Porous silicon layers

Three essential parameters are used to optimize the antireflection properties of porous silicon: the HF concentration in the ethanol, the current density and the anodization time. In our case two solutions are used: HF (48%):C_2H_5OH = 3:1 or 4:1 in volume. To adjust the adequate refractive index of the PS, the current density is fixed at 20 mA/cm^2, and the thickness of the layer is controlled by the anodization duration. Fig. 1 shows that the variation of the thicknesses according to the anodization time is exponential in nature, and that the thicknesses are very sensitive to the variations of the anodization time. We can also notice that the average growth kinetics is around 14 nm/s in our range of thicknesses. Our calculations showed that the optimum thickness of the antireflection coating (ARC PS) is 80 nm, which corresponds to 6 s of anodization.

The reflectivity curves of the PS grown on the diffused emitter with a current density of 20 mA/cm^2 and in electrolyte concentrations HF/C_2H_5OH of 3:1 and 4:1 are represented in Fig. 2. The best reflectance is obtained with the second solution, and presents an effective reflectivity of 9% with a minimum ($R \sim 0$) at the wavelength of 650 nm. This solution allows to obtain the expected value of porosity which leads exactly to the adequate refractive index, leading to the optimization of ARC PS layer. The effective reflectivity compared to that of the standard ARC nitride ($R = NH_3/SiH_4 = 5$) is improved by 1.5% absolute.

The Bruggeman effective medium approximation (EMA) is commonly used to determine the refractive indexes of inhomogeneous film [25,26]. Using this model, we consider the PS layer as an isotropic physical mixture of two components: bulk Silicon and vacuum pores smaller than the light wavelength λ [27]. Several authors have characterized thin porous silicon layer formed in the n$^+$ region of a n$^+$/p structure by SEM and AFM, and have obtained the mean size of the pores between 20 and 30 nm [7]. This justifies the use of EMA model for ellipsometry analysis, the refractive indexes for PS is thus calculated by a combination of polycrystalline-silicon (pc-Si) and void. Silicon dioxide (SiO_2) is used for the native oxide present on the surface of the PS [9]. Fig. 3 shows that there is a good agreement between the experimental and the theoretical values of reflectivity for 80 nm-thick PS layer with a porosity of 60%, covered by a thin silicon dioxide (SiO_2) layer (5–6 nm). Slight reflectivity increase in the experimental reflectivity spectrum near 1000 nm is due to the reflection on the back side of the wafer (250 μm thick). The spectroscopic ellipsometry (S.E.) measurement (Psi and Delta) carried out on these samples, and the fit based on the models proposed by Prabakaran and Strehlke [9,28], confirm an optimum reflectivity adjustment.

3.2. SiO_x/PS layers stack

In order to improve the reflectivity of a single ARC PS, a double PS layer can be grown on the top of the silicon n$^+$/p junction. However this kind of coating can lead to a degradation of the n$^+$ emitter by reducing its thickness, and degrades the surface passivation. The deposition of a silicon oxide (SiO_x) layer over the PS layer may be an alternative solution. Our PECVD system can deposit

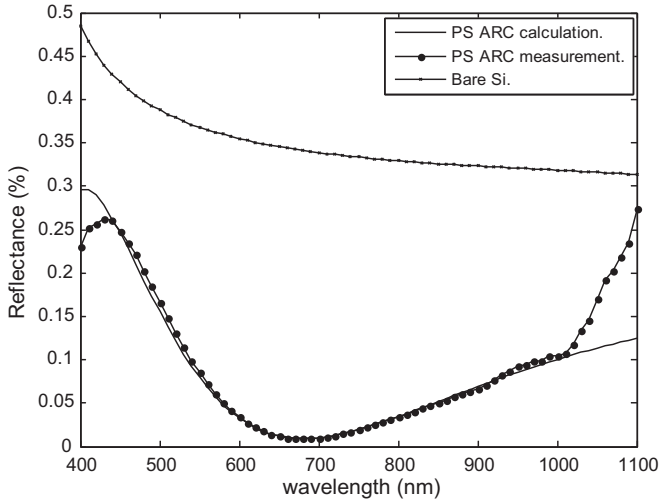

Fig. 3. Calculation and experimental reflectance spectra of PS layer ARC grown on n^+/p junction.

SiO_x layer with a refractive index $n = 1.47$ (at $\lambda = 633$ nm), and a very weak absorption in the range 300–1100 nm ($k = 0$). Such SiO_x layer can thus be used on the top of the PS layer, to realize the refractive indexes adaptation between the PS layer and the air, for antireflection optimization.

The PS layer parameters were fixed at the optimized values ($E = 80$ nm, $P = 60\%$), and the optical indexes of the SiO_x were determined by spectroscopic ellipsometry. The reflectivity of the double structure PS/SiO_x based on these parameters was computed, and led to different optimum SiO_x thicknesses: 105 nm, 90 nm, and 70 nm. The experimental reflectivity curves are presented in Fig. 4. The effective reflectance calculated from the reflectance spectra 400–1100 nm (inset in Fig. 4), varies linearly as a function of the SiO_x thickness. This result shows that the oxide film thickness of 105 nm deposited on PS layer ARC, compared to the single layer PS ARC, improves the reflectivity of 55% leading to an effective reflectance of 3.8%.

Strehlke et al. have reduced the effective reflectivity to 2.7% for double layers PS ARC with a total thickness of 160 nm in the range 400–1000 nm [29]. However such a thickness of PS may risk to degrade the properties of the underlying n^+ emitter of the solar cell, which is generally 300 nm-thick. On the other hand the best

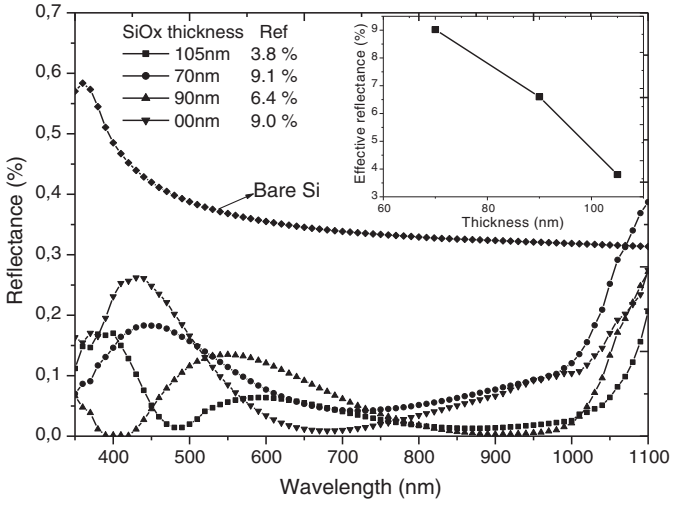

Fig. 4. Reflectance spectra of SiO_x/PS films on n^+/p junction for various thicknesses SiO_x (inset of plot: effective reflectance versus different SiO_x layers thicknesses).

Table 1
Photocurrent calculated by PC1D for different PS/SiO_x ARC structures.

Samples	Reference (%)	J_{sc} (mA/cm^2)	$\Delta J_{sc}/J_{sc}$ (%)
SiN (reference)	9.4	33.3	–
PS	9.0	32.6	−2.1
PS/SiO_x (105 nm)	3.8	33.7	1.2
PS/SiO_x (90 nm)	6.4	33.3	0.0
PS/SiO_x (70 nm)	9.1	32.7	−1.8

result obtained in the literature for a double SiN_x/SiO_x ARC layer on polished silicon is $R_{ef} = 6.3\%$ in the range $\lambda = 400$–1000 nm [21,22].

3.3. Photocurrent calculation

Following these results, the PC1D software from UNSW [24] was used to estimate the values of the photocurrent related to the antireflection properties of PS/SiO_x layers. We considered that the majority of the photons absorbed in the porous Si layer do not contribute to the photogenerated current. The cell structure parameters used for the simulation are: wafer thickness = 220 μm, resistivity = 2.5 Ω cm, emitter: N-type, 3×10^{20} cm^{-3} and surface recombination velocity = 5×10^4 cm/s. No effect related to the surface passivation degradation by the PS layer is taken into account at this step of the simulation.

To calculate the short-circuit current one must take into account the effective transmittance of the PS/SiO_x stack ($T = 1 - R - A$) calculated for each structures. The photocurrent values presented in Table 1 are compared with the standard ARC SiN. They show an improvement of 1.2% for the PS/SiO_x (105 nm), due to the lower reflectivity. However the photocurrent for PS and PS/SiO_x (70 nm) structures decrease by means of 1.8%. This can be explained essentially by two reasons: first, the great absorption of PS and the relatively higher reflectivity of the PS/SiO_x (70 nm).

4. Surface passivation results

We have shown that the reflectivity obtained with PS/SiO_x double layers is good, and can lead to an increase in the photogenerated current. We also studied the effect of such a structure on the electrical performance of the solar cell. The photovoltaic pseudo-parameters V_{oc} and FF obtained with our different structures are presented in Fig. 5. The PS layers increase the surface recombination velocity of minority carriers, leading to a large decrease of the V_{oc}. The simulation of the cell as described in Section 3.3 leads to a V_{oc} of 580 mV. With the PS layer the V_{oc} measurement decreases to 461 mV, demonstrating the strong increase of the surface recombination velocity. This effect cannot be attributed to the reduction of the emitter thickness, since this parameter has few impacts on the V_{oc}, as verified by PC1D simulation. The deposition of the SiO_x film

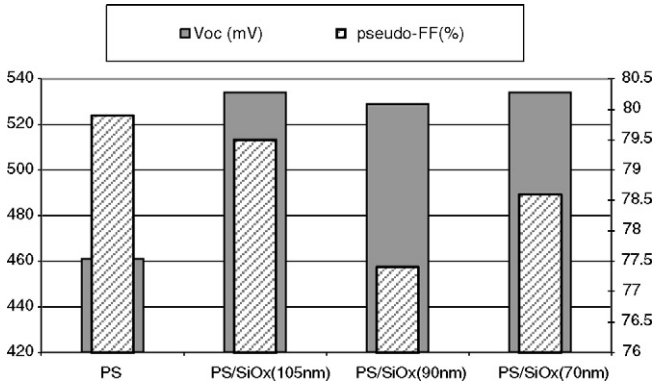

Fig. 5. Parameters suns-V_{oc} obtained in a junction n^+/p with PS and PS/SiO_x as ARC.

on the PS layer partly restores the surface passivation, leading an increase of V_{oc} from 461 mV to 536 mV. This improvement can be explained firstly by the presence of the Si–O bonds which passivates the dangling bond within PS [30,31]. The SiO_x also contains around 4at.% of hydrogen [32], which diffuses within the PS–Si layer and increases the number of Si–H bonds which is initially formed during the formation of PS [16], thus enhancing the surface passivation of the pores. The V_{oc} values are thus partly restored, but remain at this point below the reference.

The value of the pseudo fill factor is of 79.9% for the PS layer, and it slightly decreases for the PS/SiO_x (105 nm-thick layer). No significant variation is observed on the pseudo-FF, indicating that the porous silicon layer does not lead to a shunting effect within the emitter. However the pseudo-FF exhibits a great degradation: 78.6% and 77.4% respectively, for PS/SiO_x (70 nm-thick layer) and PS/SiO_x (90 nm-thick layer), indicating an increase of the shunting losses, due probably to the cut laser carried out on the edges of the round surface bounding the porous silicon. This process requires consequently a better optimization of its parameters.

5. Conclusion

The deposition of the ARC SiO_x on porous layer led to promising results. Investigations of the reflection spectra and the passivation characteristics showed that optimum results can be obtained with electrochemical anodization of PS and RF-PECVD of SiO_x ARC layers. The combination of the layers led to an improvement in the effective reflectivity of 55%, comparing to the PS layer alone. The SiO_x layer allowed also to increase the surface passivation of the PS layer, partly restoring the V_{oc} value towards the value of a standard cell. In perspective, the combination of the PS/SiO_x layer might be an alternative to the classical texturation/silicon combination. Further improvement is needed to improve the surface of the porous silicon.

Acknowledgments

The authors would like to thank the staff from the NanoLyon technical platform for helping in the realization of the structures.

References

[1] A. Prasad, S. Balakrishnan, S.K. Jain, G.C. Jain, J. Electrochem. Soc. 192 (1982) 596–598.
[2] G. Smestad, M. Kunst, C. Vial, Solar Energy Mater. Solar Cells 26 (1992) 277–283.
[3] Y.S. Tsu, Y. Xiao, M.J. Heben, X. Wu, F.J. Pern, S.K. Deb, Conf. Rec. 23rd IEEE PVSC, 1993, pp. 287–293.
[4] R.R. Bilyalov, L. Stalmans, L. Schirone, C. Lévy-Clément, IEEE Trans. Electron Dev. 46 (1999) 2035–2036.
[5] C. Peckering, M.I.J. Beale, D.J. Robbins, P.J. Pearson, R. Greef, J. Phys. C: Solid State Phys. 17 (1984) 6335.
[6] R.R.R. Bilyalov, R. Lüdemann, W. Wettling, L. Stalmans, J. Poortmans, J. Nijs, L. Schirone, G. Sotgiu, S. Strehlke, C. Lévy-Clément, Solar Energy Mater. Solar Cells 60 (2000) 391–420.
[7] P. Vitanov, M. Delibasheva, E. Goranova, M. Peneva, Solar Energy Mater. Solar Cells 61 (2000) 213.
[8] P. Vitanov, M. Goranova, N. Tyutyundzhiev, M. Delibasheva, E. Goranova, P. Peneva, Thin Solid Films 279 (1997) 299–303.
[9] S. Strehlke, S. Bastide, O. Polgar, M. Fried, C. Lévy-Clément, J. Electrochem. Soc. 147 (2000) 636–641.
[10] W. Theiss, S. Hilbrich, R. Arens-Fisher, M.G. Berger, H. Munder, in: G. Amato, C. Delerue, H.J. von Bardeleben (Eds.), Structural and Optical Properties of Porous Silicon Nanostructures, vol. 5, Gordon and Breach, London, 1997.
[11] D.W. Boeringer, R. Tsu, Appl. Phys. Lett. 65 (1994) 2332.
[12] B. Wang, D. Wang, L. Zhang, T. Li, Thin Solid Films 293 (1997) 40.
[13] A. Gupta, V.K. Jain, C.R. Jalwania, G.K. Singhal, O.P. Arora, P.P. Puri, R. Singh, M. Pal, V. Kumar, Semicond. Sci. Technol. 10 (1995) 698–702.
[14] V.M. Aroutiounian, K.H. Martirosyan, P. Soukiassian, J. Phys. D: Appl. Phys. 37 (2004) L25–L28.
[15] A. Venkateswara, F. Ozanam, J.N. Chazalviel, Electrochem. Soc. 138 (1991) 153.
[16] R. Guerrero-Lemus, F. Ben-Hander, C. Hernàndez- Rodríguez, J.M. Martinez-Duart, Mater. Sci. Eng. B 101 (2003) 249–254.
[17] C. Paillard, V. Paillard, A. Gagnaire, J. Joseph, J. Non-Cryst. Solids 216 (1997) 77–82.
[18] P. Panek, K. Drabczyk, A. Focsa, A. Slaoui, Mater. Sci. Eng. B 165 (2009) 64–66.
[19] J. Dupuis, E. Fourmond, J.F. Lelièvre, D. Ballutaud, M. Lemiti, Thin Solid Films 516 (2008) 6954–6958.
[20] I. Jozwik, P. Papet, A. Kaminski, E. Fourmond, F. Calmon, M. Lemiti, J. Non-Cryst. Solids 354 (2008) 4341–4344.
[21] K.L. Jiao, W.A. Anderson, Solar Cells 22 (1987) 229–236.
[22] J. Dupuis, J.-F. Lelièvre, E. Fourmond, V. Mong-The Yen, O. Nichiporuk, N. Le Quang, M. Lemiti, 24th European Photovoltaic Solar Energy Conference, Hamburg, Germany, September 21–25, 2009.
[23] M. Born, E. Wolf, Principles of Optics, Pergamon Press, 1970.
[24] D.A. Clugston, P.A. Basore, Photovoltaic Specialists Conference, Conference Record of the Twenty-Sixth IEEE, (1997) 207–210.
[25] L. Gao, J.Z. Gu, J. Phys. D: Appl. Phys. 35 (2002) 267–327.
[26] C. Martinet, V. Paillard, A. Gagnaire, J. Joseph, J. Non-Cryst. Solids 216 (1997) 77–82.
[27] E.V. Astrova, V.A. Tolmachev, Mater. Sci. Eng. B 69–70 (2000) 142–148.
[28] R. Prabakaran, G. Raghavan, S. Tripura Sundari, R. Kesavamoorthy, Physica E 15 (2002) 243–251.
[29] S. Strehlke, S. Bastide, J. Guillet, C. Lévy-Clément, Mater. Sci. Eng. B 69–70 (2001) 81–86.
[30] B. Gonzàlez-Díaz, R. guerrero-Lemus, J. Méndez-Ramos, B. Díaz-Herrera, V.D. Rodríguez, Sens. Actuators A: Phys. 150 (2009) 87–101.
[31] Z.H. Xiong, L.S. Liao, S. Yuan, Z.R. Yang, X.M. Ding, X.Y. Hou, Thin Solid Films 388 (2001) 271–276.
[32] J. Dupuis, Ph.D. Thesis, INSA-Lyon, France, 2009.